Acta Cryst E CRYSTALLOGRAPHIC COMMUNICATIONS

ISSN 2056-9890

Crystal structure of bis{3-(benzo[*d*][1,3]dioxol-5-yl)-5-[6-(1*H*-pyrazol-1-yl)pyridin-2-yl]-4*H*-1,2,4-triazol-4-ido}nickel(II) methanol disolvate

Kateryna Znovjyak,[a]* Sergiu Shova,[b] Vazghen Nikolian,[c] Andrii Khairulin,[d] Igor O. Fritsky,[a] Sergey O. Malinkin[a] and Maksym Seredyuk[a]

[a]Department of Chemistry, Taras Shevchenko National University of Kyiv, Volodymyrska Street 64, Kyiv, 01601, Ukraine, [b]Department of Inorganic Polymers, "Petru Poni" Institute of Macromolecular, Chemistry, Romanian Academy of Science, Aleea Grigore Ghica Voda 41-A, Iasi, 700487, Romania, [c]WimbleAI Inc., 548 Market Street, Unit 55559, San Francisco, California, USA, and [d]ChemBioCenter, Kyiv National Taras Shevchenko University, Kyiv 02094, 61 Winston Churchill Street, Ukraine. *Correspondence e-mail: znovkat@yahoo.com

Received 21 July 2025
Accepted 30 July 2025

Edited by C. Schulzke, Universität Greifswald, Germany

Keywords: crystal structure; nickel(II) complexes; neutral complexes; tridentate ligands.

CCDC reference: 2477384

Supporting information: this article has supporting information at journals.iucr.org/e

The unit cell of the title compound, $[Ni(C_{17}H_{11}N_6O_2)_2]\cdot 2CH_3OH$, consists of a neutral complex and two methanol molecules. In the complex, the two tridentate 2-[3-(benzo[*d*][1,3]dioxol-5-yl)-1*H*-1,2,4-triazol-5-yl]-6-(1*H*-pyrazol-1-yl)pyridine ligands coordinate to the central Ni^{II} ion through nitrogen atoms of the pyrazole, pyridine and triazole groups, forming a pseudooctahedral coordination sphere. Neighbouring molecules are linked through weak C—H(pz)···π(ph) interactions into monoperiodic chains, which are further linked through weak C–H···H/N/C interactions into diperiodic layers. The intermolecular contacts were quantified using Hirshfeld surface analysis and two-dimensional fingerprint plots, revealing the relative contributions of the contacts to the crystal packing to be H···H 38.4%, C···H/H···C 25.3%, N···H/H···N 14.1%, and O···H/H···O 11.8%. The average Ni—N bond distance is 2.085 Å. Energy framework analysis at the HF/3–21 G theory level was performed to quantify the interaction energies in the crystal structure.

1. Chemical context

A broad class of coordination compounds is represented by 3*d*-metal complexes based on tridentate bisazolepyridine ligands (Halcrow *et al.*, 2019; Suryadevara *et al.*, 2022), which find application in many fields, for example in catalysis (Xing *et al.*, 2014; Wei *et al.*, 2015) and molecular magnetism (Suryadevara *et al.*, 2022). In the case of asymmetric ligand design, where one of the azole groups carries a hydrogen on a nitrogen heteroatom and acts as a Brønsted acid, deprotonation can produce neutral complexes (Seredyuk *et al.*, 2014; Grunwald *et al.*, 2023). The periphery of the molecule, *i.e.* ligand substituents, also plays an important role, determining the way the molecules interact with each other, influencing the intermolecular connectivity, interaction energy and the organization of the structure.

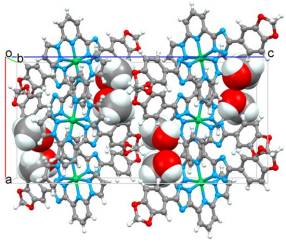

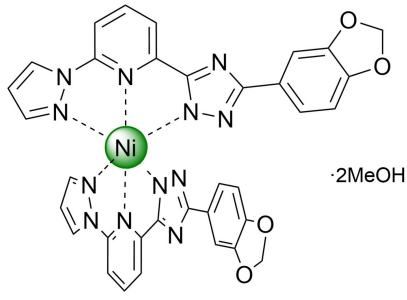

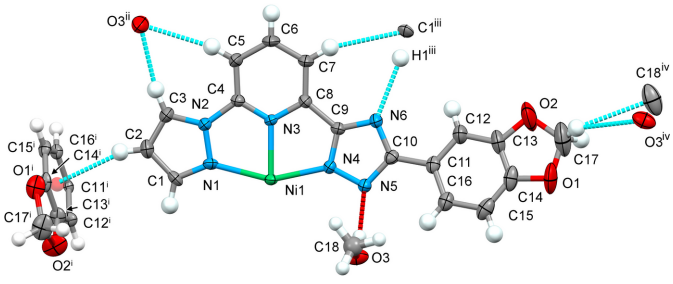

Figure 1
The molecular structure in the asymmetric unit of the title compound and contact atoms with displacement ellipsoids drawn at the 50% probability level. The strong O—H···N (red) and weak C–H···N/C/O (cyan) hydrogen bonds are shown with the nearest neighbours. Symmetry codes: (i) $1-x, 1+y, \frac{3}{2}-z$; (ii) $-\frac{1}{2}+x, \frac{1}{2}+y, \frac{3}{2}-z$; (iii) $\frac{1}{2}+x, -\frac{1}{2}+y, \frac{3}{2}-z$; (iv) $-\frac{1}{2}+x, \frac{1}{2}-y, 1-z$.

Encouraged by our results in spin-transition complexes of 3*d*-metals formed by N-heterocyclic ligands (Seredyuk *et al.*, 2006, 2007*a*,*b*, 2024*a*; Piñeiro-López *et al.*, 2018), we report here a new neutral Ni^{II} complex based on the asymmetric deprotonated ligand 2-[3-(benzo[*d*][1,3]dioxol-5-yl)-1*H*-1,2,4-triazol-5-yl)-6-(1*H*-pyrazol-1-yl]pyridine, which continues our lasting project on the study of 3*d*-metal complexes of bisazolepyridines and related organic polydentate ligands.

2. Structural commentary

The complex has a conical structure with the nickel(II) residing on twofold rotation axis and half of the formula in the asymmetric unit. The phenyl ring of the benzodioxole moiety of the ligand is rotated by 18.6 (1)° relative to the almost planar pyrazole-pyridine-triazole (pz-py-trz) fragment. The independent methanol molecule forms an O—H···N hydrogen bond with the trz ring of the ligand molecule (Fig. 1). The central Ni ion of the complex has a distorted octahedral N_6 coordination environment formed by the nitrogen donor atoms of the two tridentate ligands. The average Ni—N bond length is 2.085 Å. Distortion indices were calculated to assess how much the coordination polyhedron deviates from ideal octahedral geometry. The average trigonal distortion parameters $\Sigma = \Sigma_1^{12}(|90 - \varphi_i|)$, where φ_i refers to the twelve *cis* angles N—Ni—N′ (Drew *et al.*, 1995), and $\Theta = \Sigma_1^{24}(|60 - \theta_i|)$, where θ_i is the angle generated by superposition of two opposite faces of an octahedron (Chang *et al.*, 1990) are 117.2 and 391.6°, respectively. The values reveal a deviation of the coordination environment from an ideal octahedron (where $\Sigma = \Theta = 0$), which is, however, in the expected range for bisazolepyridine and similar ligands (see below). The calculated continuous shape measure [CShM(O_h)] value relative to the ideal octahedral symmetry is 3.599 (Kershaw Cook *et al.*, 2015). The volume of the [NiN_6] coordination polyhedron is 11.431 $Å^3$.

3. Supramolecular features

Owing to the small head-group and large planar substituent at the tail, adjacent complex molecules are interlocked and interact *via* a weak, off-centre, almost perpendicular (83.6°) C—H(pz)···π(ph) intermolecular contact between the pyrazole (pz) and phenyl (ph) groups with distances H2/C2···C_g(ph) = 2.68/3.580 (4) Å. The formed monoperiodic supramolecular chains extend along the *b*-axis direction with the stacking periodicity equal to 10.4956 (4) Å (= cell parameter *b*) (Fig. 2). Through weak intermolecular C—H(pz, py)···N/C interactions in the range 3.270 (4)–3.732 (5) Å

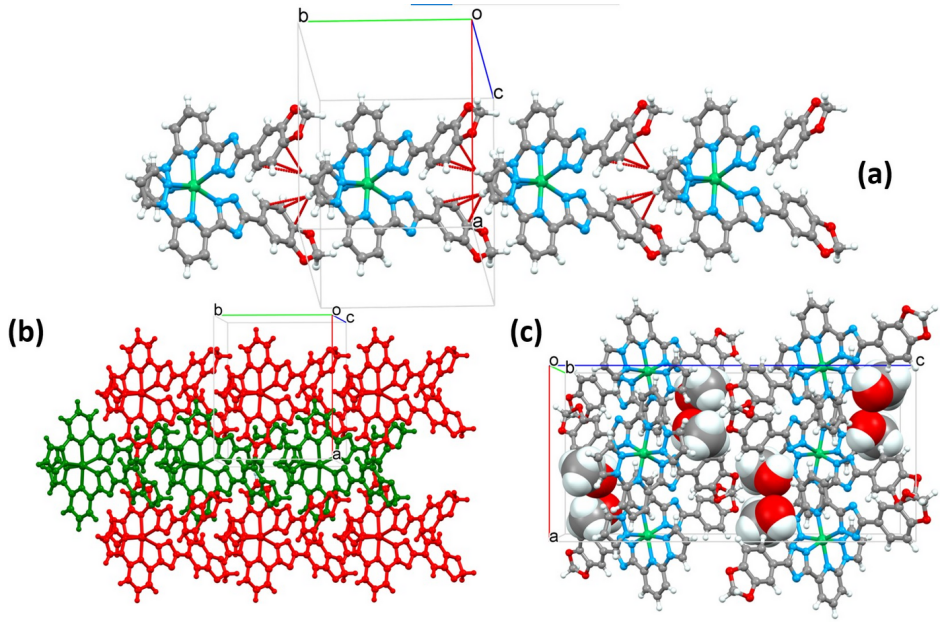

Figure 2
(*a*) A fragment of monoperiodic supramolecular column formed by stacking of molecules along the *b* axis; (*b*) supramolecular diperiodic layers formed by stacking of the supramolecular columns in the *ab* plane (for a better representation, each column has a different colour); (*c*) stacking of the diperiodic layers along the *b*-axis direction with the methanol molecules in the voids.

Table 1
Hydrogen-bond geometry (Å, °).

D—H···A	D—H	H···A	D···A	D—H···A
C3—H3···O3^{i}	0.95	2.35	3.282 (5)	165
C5—H5···O3^{i}	0.95	2.57	3.505 (4)	167
C7—H7···C1^{ii}	0.95	2.68	3.605 (5)	163
C1—H1···N6^{iii}	0.95	2.33	3.270 (4)	170
C17—H17*A*···C18^{iv}	0.99	2.78	3.479 (7)	129
C17—H17*A*···O3^{iv}	0.99	2.68	3.550 (6)	147
O3—H3*A*···N5	0.82 (4)	1.94 (4)	2.752 (4)	173 (4)

Symmetry codes: (i) $x-\frac{1}{2}, y+\frac{1}{2}, -z+\frac{3}{2}$; (ii) $x-\frac{1}{2}, y-\frac{1}{2}, -z+\frac{3}{2}$; (iii) $x+\frac{1}{2}, y+\frac{1}{2}, -z+\frac{3}{2}$; (iv) $x-\frac{1}{2}, -y+\frac{1}{2}, -z+1$.

(Table 1), neighbouring chains are joined into corrugated diperiodic layers in the *ab* plane. The layers stack without strong interlayer interactions below the van der Waals radii; however, the solvent molecules occupying voids between the layers participate in the bonding between separate layers. The methanol molecule forms a strong O—H···N hydrogen bond with the deprotonated trz group and weak C—H···O hydrogen bonds with the CH_2 group of the benzodioxole moiety belonging to a molecule in a neighbouring chain. A list of the considered hydrogen-bonding intermolecular interactions is provided in Table 1.

A Hirshfeld surface analysis was performed and the associated two-dimensional fingerprint plots were generated using *CrystalExplorer 21.5* (Spackman *et al.*, 2021), with a standard resolution of the three-dimensional d_{norm} surfaces (Fig. 3*a*). The pale-red spots symbolize short contacts and negative d_{norm} values on the surface corresponding to the interactions described above. The electrostatic potential energy calculated using the HF/3-21G basis set is mapped on the Hirshfeld surface (Fig. 3*b*). The negative charge localizes on the trz-ph moieties of the molecules, while the pz-py moieties are relatively positively charged. The two-dimensional fingerprint plots, with their relative contributions to the Hirshfeld surface mapped over d_{norm}, are shown for the H···H, C···H/H···C, N···H/H···N and O···H/H···O contacts in Fig. 4. At 38.4%, the largest contribution to the overall crystal packing is from H···H interactions, which are located in the middle region of the fingerprint plot. C···H/H···C contacts contribute 25.3%,

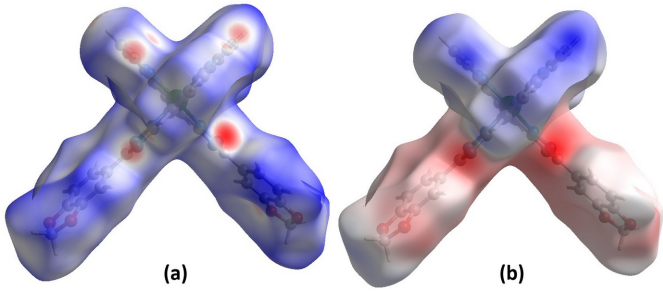

Figure 3
(*a*) A projection of d_{norm} mapped on the Hirshfeld surface identifying contact points or areas for intermolecular interactions on the molecule. Red/blue and white areas represent regions where contacts are shorter/larger than the sum and close to the sum of the van der Waals radii, respectively. (*b*) Electrostatic potential for the title compound mapped on the Hirshfeld surface. Red/blue and white areas represent regions where the charge is negative/positive or close to zero.

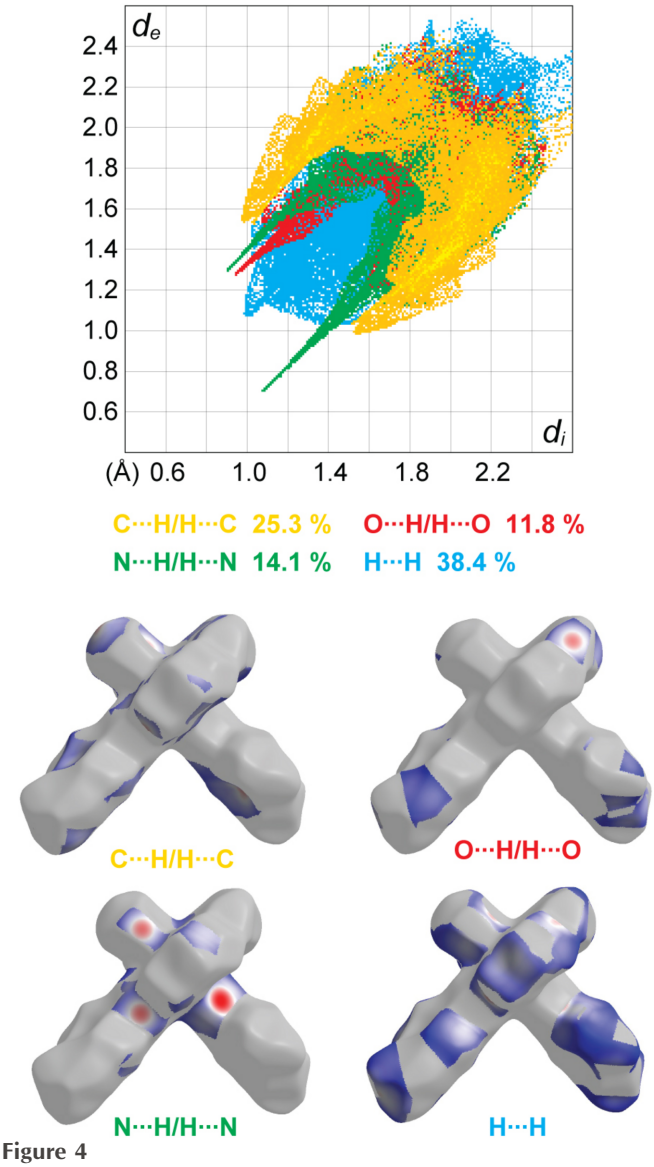

Figure 4
(*a*) Decomposition of the two-dimensional fingerprint plot into specific interactions. (*b*) A projection of d_{norm} mapped on the Hirshfeld surfaces, showing the specific intermolecular interactions on the molecule.

and O···H/H···O 11.8%, resulting in pairs of characteristic wings. The N···H/H···N contacts, represented by a pair of sharp spikes in the fingerprint plot, make a 14.1% contribution to the surface.

The energy framework (Spackman *et al.*, 2021), calculated using the wave function at the HF/3-21G theory level, including the electrostatic (E_{ele}), polarization (E_{pol}), dispersion (E_{dis}), repulsion (E_{rep}) forces, and the total energy diagrams (E_{tot}), is shown in Fig. 5. The cylindrical radii, adjusted to the same scale factor of 100, are proportional to the relative strength of the corresponding energies. The major contribution is due to dispersion forces (E_{dis}), reflecting dominating interactions in the crystal of the neutral molecules. The topology of the energy framework resembles the topology of the interactions within and between layers described above. The calculated value E_{tot} for the intrachain interaction is −50.5 kJ mol^{-1}, and for interchain interactions is down to

−95.8 kJ mol^{-1}. The interlayer interactions are represented by an energy of −19.8 kJ mol^{-1}. The colour-coded interaction mappings within a radius of 3.8 Å of a central reference molecule together with full details of the various contributions to the total energy (E_{ele}, E_{pol}, E_{dis}, E_{rep}) are shown in the table in Fig. 5.

4. Database survey

A search of the Cambridge Structural Database (CSD, Version 5.42, last update August 2024; Groom *et al.*, 2016) reveals several similar neutral 3*d* M^{II} complexes with tridentate bisazolpyridine ligands with a deprotonable azole groups, for example, of Ni^{II}: YOCFAZ (Yuan *et al.*, 2014), ZOCKOT (Xing *et al.*, 2014), and ZOTVIP (Wei *et al.*, 2015); of Fe^{II}: EGIDIL (Seredyuk *et al.*, 2024*b*), LUTGEO (Senthil Kumar *et al.*, 2015), and XODCEB (Shiga *et al.*, 2019). In addition, there are related complexes based on phenanthroline-benzimidazole (DOMQUT; Seredyuk *et al.*, 2014), dipyridylpyrrol (NIRLOT; Grunwald *et al.*, 2023). The values of the trigonal distortion and CShM(O_h) change in correspondence to the length of *M*—N distances, and for shorter distances they are systematically lower than for the longer distances. Table 2 collates some key structural parameters of the complexes and of the title compound.

Table 2
Computed distortion indices for the title compound and for similar complexes reported in the literature.

CSD Refcode	Metal ion<	<*M*—N> (Å)	Σ (°)	Θ (°)	CShM(O_h)
Title compound	Ni	2.085	117.2	391.6	3.60
YOCFAZ	Ni	2.088[a]	120.8[a]	397.6[a]	3.65[a]
ZOCKOT	Ni	2.086	121.0	375.9	3.78
ZOTVIP	Ni	2.110	124.9	382.4	3.55
EGIDIL	Fe	1.955	89.8	314.6	2.25
EGIDIL02	Fe	2.167	146.8	492.8	5.28
LUTGEO	Fe	1.933	85.0	309.6	2.10
XODCEB	Fe	1.950	87.4	276.6	1.93
DOMQUT	Fe	1.991	88.5	320.0	2.48
DOMQUT02	Fe	2.183	139.6	486.9	5.31
NIRLOT	Fe	1.939	77.3	255.6	1.68

Note: (*a*) average value.

5. Synthesis and crystallization

The synthesis of the title compound is identical to that reported for a similar complex (Seredyuk *et al.*, 2022). It was produced by using a layering technique in a standard test tube. The layering sequence was as follows: the bottom layer contained a solution of [Ni(L_2)](ClO_4)$_2$ prepared by dissolving *L* = 2-[3-(benzo[*d*][1,3]dioxol-5-yl)-1*H*-1,2,4-triazol-5-yl]-6-(1*H*-pyrazol-1-yl)pyridine (88 mg, 0.274 mmol) and Ni(ClO_4)$_2$·6H_2O (50 mg, 0.137 mmol) in boiling acetone (5 ml), to which chloroform (5 ml) was then added. The

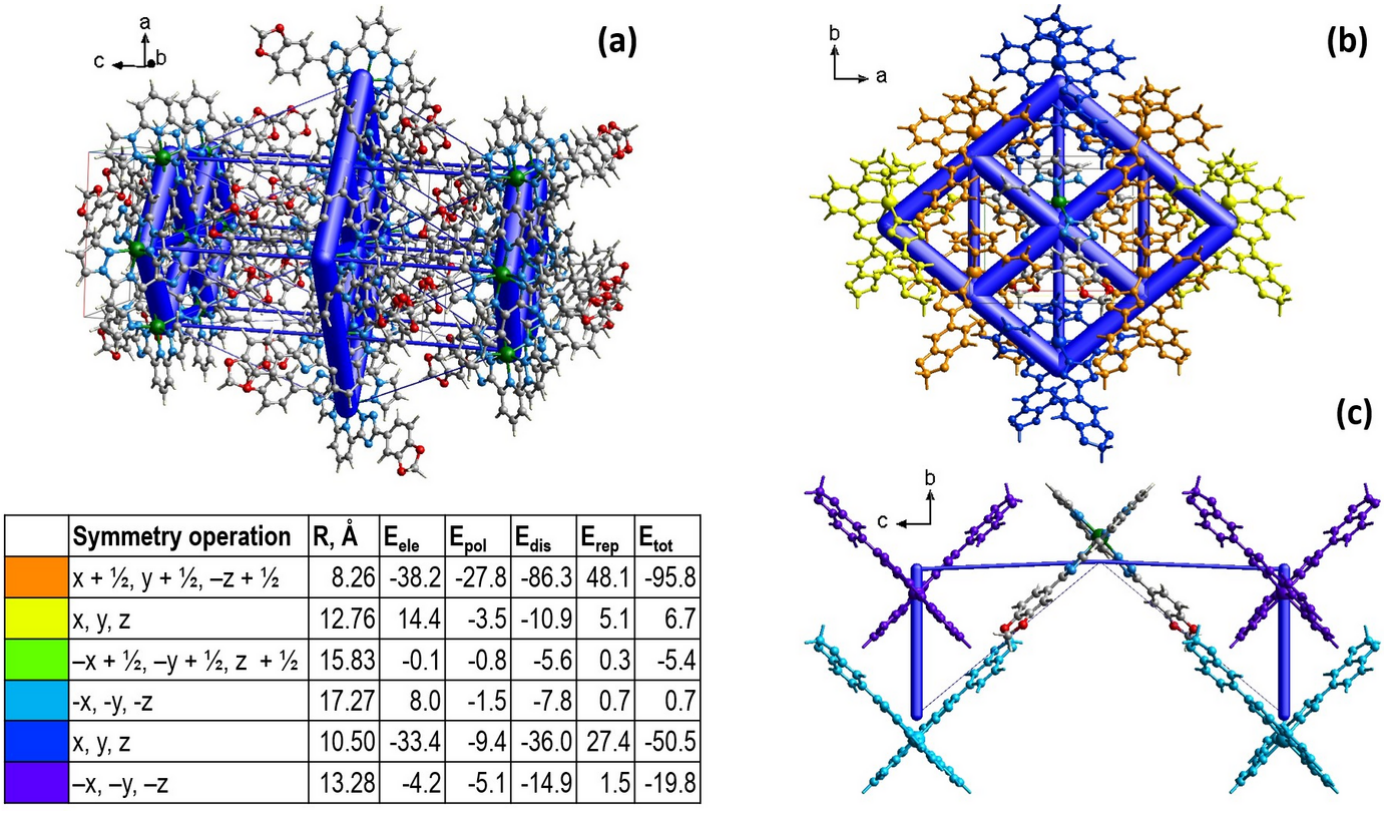

	Symmetry operation	R, Å	E_{ele}	E_{pol}	E_{dis}	E_{rep}	E_{tot}
	x + ½, y + ½, −z + ½	8.26	-38.2	-27.8	-86.3	48.1	-95.8
	x, y, z	12.76	14.4	-3.5	-10.9	5.1	6.7
	−x + ½, −y + ½, z + ½	15.83	-0.1	-0.8	-5.6	0.3	-5.4
	-x, -y, -z	17.27	8.0	-1.5	-7.8	0.7	0.7
	x, y, z	10.50	-33.4	-9.4	-36.0	27.4	-50.5
	−x, −y, −z	13.28	-4.2	-5.1	-14.9	1.5	-19.8

Figure 5
(*a*) The calculated energy frameworks, showing the total energy diagrams (E_{tot}), (*b*) decomposition of the energy framework into the part corresponding to the interactions within a supramolecular layer and (*c*) interlayer interactions. In the table, the corresponding colour-coded energy values E_{tot} are provided, including their E_{ele}, E_{pol}, E_{dis}, and E_{rep} components. Tube size is set at 100 scale.

middle layer was a methanol–chloroform mixture (1:10) (10 ml), which was covered by a layer of methanol (10 ml) to which 100 µl of NEt_3 were added dropwise. The tube was sealed and violet plate-like single crystals appeared after 2 weeks (yield *ca*. 58%). Elemental analysis calculated for $C_{36}H_{30}N_{12}NiO_6$: C, 55.05; H, 3.85; N, 21.40. Found: C, 55.66; H, 3.48; N, 21.61.

6. Refinement details

Crystal data, data collection and structure refinement details are summarized in Table 3. The O-bound H atom was refined with $U_{iso}(H) = 1.5U_{eq}(O)$; the hydrogen atom H3*A* was refined freely. All other H atoms were refined as riding [C—H = 0.95–0.99 Å with $U_{iso}(H) = 1.2–1.5U_{eq}(C)$]. An attempt to model a potential disorder in the oxalan moiety was unsuccessful as it did not improve the refinement. One reflection (002), which was obscured by the beamstop, was omitted as clear outlier.

Table 3
Experimental details.

Crystal data	
Chemical formula	$[Ni(C_{17}H_{11}N_6O_2)_2]\cdot 2CH_4O$
M_r	785.42
Crystal system, space group	Orthorhombic, *Pbcn*
Temperature (K)	200
a, *b*, *c* (Å)	12.7636 (4), 10.4956 (4), 26.5411 (12)
V (Å^3)	3555.5 (2)
Z	4
Radiation type	Mo *Kα*
μ (mm^{-1})	0.61
Crystal size (mm)	0.3 × 0.25 × 0.04
Data collection	
Diffractometer	Xcalibur, Eos
Absorption correction	Multi-scan (*CrysAlis PRO*; Rigaku OD, 2024)
T_{min}, T_{max}	0.982, 1.000
No. of measured, independent and observed [$I > 2\sigma(I)$] reflections	12665, 3146, 2236
R_{int}	0.060
$(\sin\theta/\lambda)_{max}$ (Å^{-1})	0.595
Refinement	
$R[F^2 > 2\sigma(F^2)]$, $wR(F^2)$, *S*	0.053, 0.098, 1.04
No. of reflections	3146
No. of parameters	254
H-atom treatment	H atoms treated by a mixture of independent and constrained refinement
$\Delta\rho_{max}$, $\Delta\rho_{min}$ (e Å^{-3})	0.31, −0.35

Computer programs: *CrysAlis PRO* (Rigaku OD, 2024), *SHELXT* (Sheldrick, 2015*a*), *SHELXL2018/3* (Sheldrick, 2015*b*) and *OLEX2* (Dolomanov *et al.*, 2009).

Acknowledgements

The authors are grateful to the FAIRE programme provided by the Cambridge Crystallographic Data Centre (CCDC) for the opportunity to use the Cambridge Structural Database (CSD) and associated software. Author contributions are as follows: Conceptualization, KZ and MS; methodology, KZ; formal analysis, AK; synthesis, SOM; single-crystal measurements, S*S*; writing (original draft), KZ; writing (review and editing of the manuscript), VN, MS; visualization and calculations, KZ, IOF; funding acquisition, MS and KZ.

Funding information

Funding for this research was provided by grant No. 24BF037-03 from the Ministry of Education and Science of Ukraine. This work was supported by the European Union's HORIZON-MSCA-2023-SE-01 programme under grant agreement No. 101183082 – PacemCAT.

References

Chang, H. R., McCusker, J. K., Toftlund, H., Wilson, S. R., Trautwein, A. X., Winkler, H. & Hendrickson, D. N. (1990). *J. Am. Chem. Soc.* **112**, 6814–6827.
Dolomanov, O. V., Bourhis, L. J., Gildea, R. J., Howard, J. A. K. & Puschmann, H. (2009). *J. Appl. Cryst.* **42**, 339–341.
Drew, M. G. B., Harding, C. J., McKee, V., Morgan, G. G. & Nelson, J. (1995). *J. Chem. Soc. Chem. Commun.* pp. 1035–1038.
Groom, C. R., Bruno, I. J., Lightfoot, M. P. & Ward, S. C. (2016). *Acta Cryst.* B**72**, 171–179.
Grunwald, J., Torres, J., Buchholz, A., Näther, C., Kämmerer, L., Gruber, M., Rohlf, S., Thakur, S., Wende, H., Plass, W., Kuch, W. & Tuczek, F. (2023). *Chem. Sci.* **14**, 7361–7380.
Halcrow, M. A., Capel Berdiell, I., Pask, C. M. & Kulmaczewski, R. (2019). *Inorg. Chem.* **58**, 9811–9821.
Kershaw Cook, L. J., Mohammed, R., Sherborne, G., Roberts, T. D., Alvarez, S. & Halcrow, M. A. (2015). *Coord. Chem. Rev.* **289–290**, 2–12.
Piñeiro-López, L., Valverde-Muñoz, F. J., Seredyuk, M., Bartual-Murgui, C., Muñoz, M. C. & Real, J. A. (2018). *Eur. J. Inorg. Chem.* pp. 289–296.
Rigaku OD (2024). *CrysAlis PRO* . Rigaku Oxford Diffraction, Yarnton, England.
Senthil Kumar, K., Šalitroš, I., Heinrich, B., Fuhr, O. & Ruben, M. (2015). *J. Mater. Chem. C.* **3**, 11635–11644.
Seredyuk, M., Gaspar, A. B., Ksenofontov, V., Reiman, S., Galyametdinov, Y., Haase, W., Rentschler, E. & Gütlich, P. (2006). *Hyperfine Interact.* **166**, 385–390.
Seredyuk, M., Gaspar, A. B., Kusz, J., Bednarek, G. & Gütlich, P. (2007*a*). *J. Appl. Cryst.* **40**, 1135–1145.
Seredyuk, M., Haukka, M., Fritsky, I. O., Kozłowski, H., Krämer, R., Pavlenko, V. A. & Gütlich, P. (2007*b*). *Dalton Trans.* pp. 3183–3194.
Seredyuk, M., Li, R., Znovjyak, K., Zhang, Z., Valverde–Muñoz, F. J., Li, B., Muñoz, M. C., Li, Q., Liu, B., Levchenko, G. & Real, J. A. (2024*a*). *Adv. Funct. Mater.* **34**, 2315487.
Seredyuk, M., Znovjyak, K., Valverde-Muñoz, F. J., da Silva, I., Muñoz, M. C., Moroz, Y. S. & Real, J. A. (2022). *J. Am. Chem. Soc.* **144**, 14297–14309.
Seredyuk, M., Znovjyak, K., Valverde-Muñoz, F. J., Muñoz, M. C., Fritsky, I. O. & Real, J. A. (2024*b*). *Dalton Trans.* **53**, 8041–8049.
Seredyuk, M., Znovjyak, K. O., Kusz, J., Nowak, M., Muñoz, M. C. & Real, J. A. (2014). *Dalton Trans.* **43**, 16387–16394.
Sheldrick, G. M. (2015*a*). *Acta Cryst.* A**71**, 3–8.
Sheldrick, G. M. (2015*b*). *Acta Cryst.* C**71**, 3–8.
Shiga, T., Saiki, R., Akiyama, L., Kumai, R., Natke, D., Renz, F., Cameron, J. M., Newton, G. N. & Oshio, H. (2019). *Angew. Chem. Int. Ed.* **58**, 5658–5662.
Spackman, P. R., Turner, M. J., McKinnon, J. J., Wolff, S. K., Grimwood, D. J., Jayatilaka, D. & Spackman, M. A. (2021). *J. Appl. Cryst.* **54**, 1006–1011.

Suryadevara, N., Mizuno, A., Spieker, L., Salamon, S., Sleziona, S., Maas, A., Pollmann, E., Heinrich, B., Schleberger, M., Wende, H., Kuppusamy, S. K. & Ruben, M. (2022). *Chem. A Eur. J.* **28**, e202103853.

Wei, S. Y., Wang, J. L., Zhang, C. S., Xu, X.-T., Zhang, X. X., Wang, J. X. & Xing, Y.-H. (2015). *ChemPlusChem* **80**, 549-558.

Xing, N., Xu, L. T., Liu, X., Wu, Q., Ma, X. T. & Xing, Y. H. (2014). *ChemPlusChem* **79**, 1198-1207.

Yuan, L.-Z., Ge, Q., Zhao, X.-F., Ouyang, Y., Li, S.-H., Xie, C.-Z. & Xu, J.-Y. (2014). *Synth. React. Inorg. Met.-Org. Nano-Met. Chem.* **44**, 1175–1182.

supporting information

Acta Cryst. (2025). E**81**, 821-826 [https://doi.org/10.1107/S2056989025006851]

Crystal structure of bis{3-(benzo[*d*][1,3]dioxol-5-yl)-5-[6-(1*H*-pyrazol-1-yl)pyridin-2-yl]-4*H*-1,2,4-triazol-4-ido}nickel(II) methanol disolvate

Kateryna Znovjyak, Sergiu Shova, Vazghen Nikolian, Andrii Khairulin, Igor O. Fritsky, Sergey O. Malinkin and Maksym Seredyuk

Computing details

Bis{3-(benzo[*d*][1,3]dioxol-5-yl)-5-[6-(1*H*-pyrazol-1-yl)pyridin-2-yl]-4*H*-1,2,4-triazol-4-ido}nickel(II) methanol disolvate

Crystal data

$[Ni(C_{17}H_{11}N_6O_2)_2]\cdot 2CH_4O$
$M_r = 785.42$
Orthorhombic, *Pbcn*
$a = 12.7636$ (4) Å
$b = 10.4956$ (4) Å
$c = 26.5411$ (12) Å
$V = 3555.5$ (2) Å^3
$Z = 4$
$F(000) = 1624$
$D_x = 1.467$ Mg m^{-3}
Mo $K\alpha$ radiation, $\lambda = 0.71073$ Å
Cell parameters from 2720 reflections
$\theta = 2.2$–$25.8°$
$\mu = 0.61$ mm^{-1}
$T = 200$ K
Plate, clear light violet
0.3 × 0.25 × 0.04 mm

Data collection

Xcalibur, Eos diffractometer
Radiation source: fine-focus sealed X-ray tube, Enhance (Mo) X-ray Source
Graphite monochromator
Detector resolution: 16.1593 pixels mm^{-1}
ω scans
Absorption correction: multi-scan (CrysAlisPro; Rigaku OD, 2024)
$T_{min} = 0.982$, $T_{max} = 1.000$
12665 measured reflections
3146 independent reflections
2236 reflections with $I > 2\sigma(I)$
$R_{int} = 0.060$
$\theta_{max} = 25.0°$, $\theta_{min} = 2.2°$
$h = -10\rightarrow15$
$k = -12\rightarrow9$
$l = -19\rightarrow31$

Refinement

Refinement on F^2
Least-squares matrix: full
$R[F^2 > 2\sigma(F^2)] = 0.053$
$wR(F^2) = 0.098$
$S = 1.04$
3146 reflections
254 parameters
0 restraints
Primary atom site location: dual
Hydrogen site location: mixed
H atoms treated by a mixture of independent and constrained refinement
$w = 1/[\sigma^2(F_o^2) + (0.0254P)^2 + 2.476P]$ where $P = (F_o^2 + 2F_c^2)/3$
$(\Delta/\sigma)_{max} < 0.001$
$\Delta\rho_{max} = 0.31$ e Å^{-3}
$\Delta\rho_{min} = -0.35$ e Å^{-3}

Special details

Geometry. All esds (except the esd in the dihedral angle between two l.s. planes) are estimated using the full covariance matrix. The cell esds are taken into account individually in the estimation of esds in distances, angles and torsion angles; correlations between esds in cell parameters are only used when they are defined by crystal symmetry. An approximate (isotropic) treatment of cell esds is used for estimating esds involving l.s. planes.

Fractional atomic coordinates and isotropic or equivalent isotropic displacement parameters (Å²)

	x	*y*	*z*	U_{iso}*/U_{eq}
Ni1	0.500000	0.69588 (5)	0.750000	0.02073 (17)
N3	0.34364 (17)	0.7067 (2)	0.76431 (9)	0.0210 (6)
N6	0.29635 (19)	0.4568 (2)	0.67333 (11)	0.0294 (7)
O3	0.6459 (2)	0.5655 (3)	0.61469 (11)	0.0479 (8)
N4	0.43894 (17)	0.5611 (2)	0.70073 (10)	0.0235 (6)
N2	0.38524 (18)	0.8644 (2)	0.81994 (10)	0.0268 (7)
N1	0.48769 (18)	0.8386 (2)	0.80741 (10)	0.0246 (6)
N5	0.47127 (18)	0.4777 (2)	0.66463 (10)	0.0262 (7)
C4	0.3065 (2)	0.7917 (3)	0.79625 (12)	0.0251 (8)
C10	0.3842 (2)	0.4172 (3)	0.64927 (13)	0.0263 (8)
C7	0.1705 (2)	0.6386 (3)	0.74627 (15)	0.0388 (10)
H7	0.123624	0.584348	0.728607	0.047*
C9	0.3345 (2)	0.5459 (3)	0.70425 (13)	0.0245 (8)
O2	0.2148 (3)	0.0879 (3)	0.54493 (14)	0.0921 (12)
C6	0.1333 (2)	0.7279 (4)	0.77975 (15)	0.0431 (11)
H6	0.059945	0.735043	0.785111	0.052*
C5	0.2007 (2)	0.8075 (3)	0.80573 (13)	0.0363 (9)
H5	0.175702	0.869689	0.828819	0.044*
C12	0.2941 (3)	0.2482 (3)	0.60018 (15)	0.0412 (10)
H12	0.234731	0.254816	0.621630	0.049*
C11	0.3833 (2)	0.3232 (3)	0.60829 (13)	0.0290 (8)
C8	0.2776 (2)	0.6292 (3)	0.73882 (12)	0.0250 (8)
C3	0.3786 (3)	0.9550 (3)	0.85594 (14)	0.0380 (10)
H3	0.316294	0.988162	0.870435	0.046*
O1	0.3599 (3)	0.0627 (3)	0.49288 (12)	0.0741 (10)
C16	0.4691 (3)	0.3094 (3)	0.57656 (13)	0.0363 (9)
H16	0.529763	0.359884	0.582264	0.044*
C14	0.3798 (3)	0.1522 (4)	0.52947 (15)	0.0462 (10)
C15	0.4686 (3)	0.2229 (3)	0.53634 (15)	0.0452 (10)
H15	0.527454	0.213721	0.514753	0.054*
C2	0.4785 (3)	0.9895 (3)	0.86743 (15)	0.0406 (10)
H2	0.499792	1.051567	0.891392	0.049*
C13	0.2950 (3)	0.1662 (4)	0.56088 (16)	0.0485 (11)
C1	0.5433 (2)	0.9155 (3)	0.83694 (13)	0.0287 (8)
H1	0.617703	0.919390	0.837224	0.034*
C18	0.6032 (4)	0.6536 (4)	0.58103 (17)	0.0741 (15)
H18A	0.570036	0.608158	0.552967	0.111*
H18B	0.658810	0.708858	0.568045	0.111*
H18C	0.550579	0.705408	0.598456	0.111*

C17	0.2564 (4)	0.0181 (5)	0.5035 (2)	0.0920 (18)
H17A	0.211247	0.029769	0.473482	0.110*
H17B	0.258379	−0.073876	0.511717	0.110*
H3A	0.597 (3)	0.534 (4)	0.6305 (15)	0.048 (13)*

Atomic displacement parameters (Å²)

	U^{11}	U^{22}	U^{33}	U^{12}	U^{13}	U^{23}
Ni1	0.0147 (3)	0.0252 (3)	0.0223 (3)	0.000	0.0005 (3)	0.000
N3	0.0162 (13)	0.0235 (14)	0.0234 (17)	0.0020 (11)	0.0026 (11)	−0.0039 (14)
N6	0.0246 (15)	0.0327 (17)	0.0310 (18)	−0.0006 (12)	−0.0024 (13)	−0.0107 (15)
O3	0.0357 (16)	0.058 (2)	0.050 (2)	0.0056 (13)	0.0075 (14)	0.0173 (17)
N4	0.0220 (15)	0.0247 (15)	0.0237 (17)	0.0005 (11)	0.0009 (12)	−0.0042 (14)
N2	0.0208 (15)	0.0291 (16)	0.0305 (18)	0.0003 (11)	0.0014 (12)	−0.0093 (15)
N1	0.0169 (14)	0.0303 (15)	0.0265 (16)	−0.0007 (11)	0.0048 (12)	0.0012 (13)
N5	0.0231 (15)	0.0283 (15)	0.0271 (18)	0.0007 (11)	−0.0004 (12)	−0.0063 (15)
C4	0.0186 (17)	0.0298 (19)	0.027 (2)	0.0004 (14)	−0.0004 (14)	−0.0028 (18)
C10	0.0264 (18)	0.0256 (19)	0.027 (2)	0.0039 (14)	−0.0006 (15)	0.0003 (18)
C7	0.0173 (18)	0.049 (2)	0.051 (3)	−0.0011 (14)	0.0014 (17)	−0.020 (2)
C9	0.0190 (18)	0.0267 (19)	0.028 (2)	−0.0011 (13)	0.0006 (14)	−0.0016 (18)
O2	0.104 (3)	0.091 (3)	0.082 (3)	−0.043 (2)	−0.005 (2)	−0.047 (2)
C6	0.0161 (18)	0.058 (3)	0.056 (3)	0.0009 (16)	0.0055 (17)	−0.019 (2)
C5	0.0253 (19)	0.046 (2)	0.038 (2)	0.0009 (16)	0.0043 (16)	−0.019 (2)
C12	0.044 (2)	0.041 (2)	0.039 (3)	−0.0047 (17)	−0.0009 (18)	−0.013 (2)
C11	0.0362 (19)	0.0242 (19)	0.027 (2)	0.0044 (14)	−0.0051 (16)	−0.0002 (18)
C8	0.0214 (17)	0.0274 (18)	0.026 (2)	−0.0009 (13)	−0.0020 (14)	−0.0039 (17)
C3	0.030 (2)	0.039 (2)	0.045 (3)	0.0021 (16)	0.0047 (17)	−0.018 (2)
O1	0.122 (3)	0.054 (2)	0.047 (2)	−0.0098 (19)	−0.0071 (19)	−0.0288 (19)
C16	0.045 (2)	0.032 (2)	0.031 (2)	0.0050 (16)	−0.0009 (17)	−0.003 (2)
C14	0.079 (3)	0.032 (2)	0.027 (2)	0.005 (2)	−0.008 (2)	−0.003 (2)
C15	0.064 (3)	0.040 (2)	0.032 (2)	0.0120 (19)	0.0068 (19)	0.000 (2)
C2	0.041 (2)	0.039 (2)	0.042 (3)	−0.0059 (17)	−0.0033 (18)	−0.017 (2)
C13	0.066 (3)	0.036 (2)	0.044 (3)	−0.0125 (19)	−0.013 (2)	−0.011 (2)
C1	0.0235 (17)	0.0300 (19)	0.033 (2)	−0.0098 (14)	−0.0064 (16)	−0.0005 (19)
C18	0.113 (4)	0.058 (3)	0.051 (3)	0.032 (3)	0.026 (3)	0.011 (3)
C17	0.143 (5)	0.065 (4)	0.069 (4)	−0.031 (4)	−0.016 (4)	−0.026 (3)

Geometric parameters (Å, º)

Ni1—N3^{i}	2.035 (2)	O2—C17	1.425 (5)
Ni1—N3	2.035 (2)	C6—H6	0.9500
Ni1—N4^{i}	2.078 (3)	C6—C5	1.383 (4)
Ni1—N4	2.078 (3)	C5—H5	0.9500
Ni1—N1	2.143 (3)	C12—H12	0.9500
Ni1—N1^{i}	2.143 (3)	C12—C11	1.401 (4)
N3—C4	1.319 (4)	C12—C13	1.353 (5)
N3—C8	1.353 (4)	C11—C16	1.389 (4)
N6—C10	1.356 (4)	C3—H3	0.9500

N6—C9	1.336 (4)	C3—C2	1.360 (4)
O3—C18	1.396 (5)	O1—C14	1.375 (4)
O3—H3A	0.82 (3)	O1—C17	1.430 (5)
N4—N5	1.362 (3)	C16—H16	0.9500
N4—C9	1.345 (3)	C16—C15	1.401 (5)
N2—N1	1.376 (3)	C14—C15	1.366 (5)
N2—C4	1.410 (4)	C14—C13	1.374 (5)
N2—C3	1.350 (4)	C15—H15	0.9500
N1—C1	1.330 (4)	C2—H2	0.9500
N5—C10	1.343 (4)	C2—C1	1.394 (5)
C4—C5	1.383 (4)	C1—H1	0.9500
C10—C11	1.468 (4)	C18—H18A	0.9800
C7—H7	0.9500	C18—H18B	0.9800
C7—C6	1.376 (5)	C18—H18C	0.9800
C7—C8	1.385 (4)	C17—H17A	0.9900
C9—C8	1.461 (4)	C17—H17B	0.9900
O2—C13	1.379 (4)		

N3^{i}—Ni1—N3	173.57 (14)	C4—C5—H5	121.8
N3—Ni1—N4	77.75 (10)	C6—C5—C4	116.3 (3)
N3—Ni1—N4^{i}	106.77 (10)	C6—C5—H5	121.8
N3^{i}—Ni1—N4	106.77 (9)	C11—C12—H12	121.0
N3^{i}—Ni1—N4^{i}	77.75 (9)	C13—C12—H12	121.0
N3—Ni1—N1	75.88 (9)	C13—C12—C11	118.0 (4)
N3—Ni1—N1^{i}	99.53 (9)	C12—C11—C10	119.8 (3)
N3^{i}—Ni1—N1^{i}	75.88 (9)	C16—C11—C10	120.9 (3)
N3^{i}—Ni1—N1	99.53 (9)	C16—C11—C12	119.3 (3)
N4—Ni1—N4^{i}	94.21 (14)	N3—C8—C7	120.0 (3)
N4—Ni1—N1	153.63 (9)	N3—C8—C9	111.4 (3)
N4^{i}—Ni1—N1^{i}	153.63 (9)	C7—C8—C9	128.6 (3)
N4—Ni1—N1^{i}	93.21 (10)	N2—C3—H3	126.6
N4^{i}—Ni1—N1	93.21 (10)	N2—C3—C2	106.7 (3)
N1—Ni1—N1^{i}	91.26 (14)	C2—C3—H3	126.6
C4—N3—Ni1	120.7 (2)	C14—O1—C17	104.8 (3)
C4—N3—C8	120.3 (3)	C11—C16—H16	119.2
C8—N3—Ni1	118.9 (2)	C11—C16—C15	121.7 (3)
C9—N6—C10	101.7 (2)	C15—C16—H16	119.2
C18—O3—H3A	107 (3)	C15—C14—O1	128.2 (4)
N5—N4—Ni1	140.06 (18)	C15—C14—C13	121.0 (4)
C9—N4—Ni1	114.1 (2)	C13—C14—O1	110.9 (4)
C9—N4—N5	105.8 (2)	C16—C15—H15	121.4
N1—N2—C4	117.6 (2)	C14—C15—C16	117.2 (4)
C3—N2—N1	111.6 (2)	C14—C15—H15	121.4
C3—N2—C4	130.7 (3)	C3—C2—H2	126.9
N2—N1—Ni1	112.28 (18)	C3—C2—C1	106.1 (3)
C1—N1—Ni1	143.5 (2)	C1—C2—H2	126.9
C1—N1—N2	104.2 (3)	C12—C13—O2	127.6 (4)
C10—N5—N4	105.5 (2)	C12—C13—C14	122.8 (4)

N3—C4—N2	113.3 (2)	C14—C13—O2	109.6 (4)
N3—C4—C5	123.3 (3)	N1—C1—C2	111.3 (3)
C5—C4—N2	123.3 (3)	N1—C1—H1	124.4
N6—C10—C11	123.3 (3)	C2—C1—H1	124.4
N5—C10—N6	113.3 (3)	O3—C18—H18A	109.5
N5—C10—C11	123.3 (3)	O3—C18—H18B	109.5
C6—C7—H7	120.6	O3—C18—H18C	109.5
C6—C7—C8	118.8 (3)	H18A—C18—H18B	109.5
C8—C7—H7	120.6	H18A—C18—H18C	109.5
N6—C9—N4	113.7 (3)	H18B—C18—H18C	109.5
N6—C9—C8	128.6 (3)	O2—C17—O1	109.1 (4)
N4—C9—C8	117.7 (3)	O2—C17—H17A	109.9
C13—O2—C17	105.5 (4)	O2—C17—H17B	109.9
C7—C6—H6	119.4	O1—C17—H17A	109.9
C7—C6—C5	121.2 (3)	O1—C17—H17B	109.9
C5—C6—H6	119.4	H17A—C17—H17B	108.3

Ni1—N3—C4—N2	−3.3 (4)	C10—C11—C16—C15	−178.1 (3)
Ni1—N3—C4—C5	176.9 (3)	C7—C6—C5—C4	−0.2 (6)
Ni1—N3—C8—C7	−177.2 (3)	C9—N6—C10—N5	0.3 (4)
Ni1—N3—C8—C9	0.9 (3)	C9—N6—C10—C11	−176.1 (3)
Ni1—N4—N5—C10	178.3 (3)	C9—N4—N5—C10	−0.6 (3)
Ni1—N4—C9—N6	−178.4 (2)	C6—C7—C8—N3	0.2 (5)
Ni1—N4—C9—C8	3.8 (4)	C6—C7—C8—C9	−177.5 (3)
Ni1—N1—C1—C2	179.5 (3)	C12—C11—C16—C15	0.4 (5)
N3—C4—C5—C6	0.3 (5)	C11—C12—C13—O2	−177.2 (4)
N6—C10—C11—C12	−15.0 (5)	C11—C12—C13—C14	1.1 (6)
N6—C10—C11—C16	163.5 (3)	C11—C16—C15—C14	0.0 (5)
N6—C9—C8—N3	179.5 (3)	C8—N3—C4—N2	179.7 (3)
N6—C9—C8—C7	−2.6 (6)	C8—N3—C4—C5	−0.1 (5)
N4—N5—C10—N6	0.2 (4)	C8—C7—C6—C5	0.0 (6)
N4—N5—C10—C11	176.5 (3)	C3—N2—N1—Ni1	−179.7 (2)
N4—C9—C8—N3	−3.1 (4)	C3—N2—N1—C1	0.3 (3)
N4—C9—C8—C7	174.8 (3)	C3—N2—C4—N3	−176.7 (3)
N2—N1—C1—C2	−0.4 (4)	C3—N2—C4—C5	3.1 (6)
N2—C4—C5—C6	−179.5 (3)	C3—C2—C1—N1	0.4 (4)
N2—C3—C2—C1	−0.2 (4)	O1—C14—C15—C16	179.4 (3)
N1—N2—C4—N3	−0.2 (4)	O1—C14—C13—O2	−1.6 (5)
N1—N2—C4—C5	179.6 (3)	O1—C14—C13—C12	179.9 (4)
N1—N2—C3—C2	−0.1 (4)	C14—O1—C17—O2	3.1 (5)
N5—N4—C9—N6	0.8 (4)	C15—C14—C13—O2	177.9 (4)
N5—N4—C9—C8	−176.9 (3)	C15—C14—C13—C12	−0.7 (6)
N5—C10—C11—C12	169.0 (3)	C13—O2—C17—O1	−4.1 (5)
N5—C10—C11—C16	−12.5 (5)	C13—C12—C11—C10	177.6 (3)
C4—N3—C8—C7	−0.1 (5)	C13—C12—C11—C16	−1.0 (5)
C4—N3—C8—C9	177.9 (3)	C13—C14—C15—C16	0.1 (6)
C4—N2—N1—Ni1	3.2 (3)	C17—O2—C13—C12	−178.1 (4)
C4—N2—N1—C1	−176.8 (3)	C17—O2—C13—C14	3.4 (5)

C4—N2—C3—C2	176.6 (3)	C17—O1—C14—C15	179.6 (4)
C10—N6—C9—N4	−0.7 (4)	C17—O1—C14—C13	−1.0 (5)
C10—N6—C9—C8	176.8 (3)		

Symmetry code: (i) −*x*+1, *y*, −*z*+3/2.

Hydrogen-bond geometry (Å, º)

D—H···*A*	*D*—H	H···*A*	*D*···*A*	*D*—H···*A*
C3—H3···O3^{ii}	0.95	2.35	3.282 (5)	165
C5—H5···O3^{ii}	0.95	2.57	3.505 (4)	167
C7—H7···C1^{iii}	0.95	2.68	3.605 (5)	163
C1—H1···N6^{iv}	0.95	2.33	3.270 (4)	170
C17—H17*A*···C18^{v}	0.99	2.78	3.479 (7)	129
C17—H17*A*···O3^{v}	0.99	2.68	3.550 (6)	147
O3—H3*A*···N5	0.82 (4)	1.94 (4)	2.752 (4)	173 (4)

Symmetry codes: (ii) *x*−1/2, *y*+1/2, −*z*+3/2; (iii) *x*−1/2, *y*−1/2, −*z*+3/2; (iv) *x*+1/2, *y*+1/2, −*z*+3/2; (v) *x*−1/2, −*y*+1/2, −*z*+1.

Hydrogen-bond geometry (Å, °).

D–H···A	***D–H***	***H···A***	***D···A***	***D–H···A***
C3–H···O3^{ii}	0.95	2.36	3.282 (5)	165
C5–H···O3^{ii}	0.95	2.57	3.505 (4)	167
C7–H···C1^{iii}	0.95	2.68	3.605 (5)	163
N6···H–C1^{iii}	0.95	2.33	3.270 (4)	170
C17–H···C18^{iv}	0.99	2.78	3.479 (7)	129
C17–H···O3^{iv}	0.99	2.68	3.550 (6)	147
O3–H···N6	0.82	1.94	2.753 (4)	172

Symmetry codes: (i) 1-x,1+y,1.5-z; (ii) -1/2+x,1/2+y,1.5-z; (iii) -1/2+x,-1/2+y,1.5-z; (iv) -1/2+x,1/2-y,1-z